Hypertension Research
https://doi.org/10.1038/s41440-025-02401-x

ARTICLE

Effects of perirenal fat accumulation on cardiometabolic and renal functions and mineralocorticoid receptor activation in primary aldosteronism

Ryunosuke Mitsuno[1] · Toshifumi Nakamura[1] · Kengo Nakamura[1] · Kenji Kaneko[1] · Daiki Kojima[1] · Yosuke Mizutani[1] · Yoshitake Yamada[2] · Masahiro Jinzaki[2] · Tatsuhiko Azegami[1] · Takeshi Kanda[3,4] · Kenichiro Kinouchi[1] · Hiroshi Itoh[5] · Jun Yoshino[1,3,4] · Kaori Hayashi[1]

Received: 16 April 2025 / Revised: 7 August 2025 / Accepted: 23 August 2025

Abstract

Perirenal fat (PRF), an ectopic fat depot lying adjacent to kidneys, is a risk factor for cardiometabolic and renal dysfunctions in patients with obesity and type 2 diabetes. We aimed to investigate the involvement of PRF in the pathophysiology and treatment of primary aldosteronism (PA). To this end, we measured PRF volume by abdominal CT and evaluated the relationships among PRF volume, cardiometabolic and renin-angiotensin-aldosterone system (RAAS) parameters, and therapeutic response to mineralocorticoid receptor antagonist (MRA) treatment in well-phenotyped PA patients. In addition, we evaluated the effects of MRA treatment on inflammation and fibrosis, potential downstream targets of MR signaling, by analyzing PRF obtained from obese (db/db) mice. PRF volume (PRF%) and visceral fat volume (VFV) were associated with various cardiometabolic and renal risk markers and RAAS parameters, such as body mass index, creatinine, triglyceride, high-density lipoprotein cholesterol, uric acid, fasting glucose, C-reactive protein, 24-h urine aldosterone, and 24-h urine normetanephrine (all $P < 0.05$). PRF%, but not VFV, positively correlated with changes in systolic and diastolic blood pressure and initial estimated glomerular filtration rate (eGFR) fall following MRA treatment after adjusting for confounders (all $P < 0.05$). In addition, MRA treatment decreased PRF expression of markers of macrophage infiltration and fibrosis in db/db mice (all $P < 0.05$). In conclusion, our results suggest that PRF accumulation is involved in the mechanisms linking MR activation to cardiometabolic and renal dysfunctions in PA patients. Moreover, PRF could be not only a prognostic factor but also a new therapeutic target for MRA-resistant hypertension.

Keywords Perirenal fat · Primary aldosteronism · Mineralocorticoid receptor antagonist (MRA) · Renin-angiotensin-aldosterone system (RAAS) · Hypertension

Introduction

Primary aldosteronism (PA) is the most common cause of endocrine hypertension that accounts for 5–20% in hypertensive patients [1–3]. PA is caused by overproduction and secretion of aldosterone, and accumulating evidence suggests that hyperaldosteronism is involved in the

Supplementary information The online version contains supplementary material available at https://doi.org/10.1038/s41440-025-02401-x.

✉ Jun Yoshino
jyoshino@med.shimane-u.ac.jp

[1] Division of Endocrinology, Metabolism and Nephrology, Department of Internal Medicine, Keio University School of Medicine, Shinjuku-ku, Tokyo, Japan

[2] Department of Radiology, Keio University School of Medicine, Shinjuku-ku, Tokyo, Japan

[3] Division of Nephrology, Department of Internal Medicine, Faculty of Medicine, Shimane University, Izumo, Shimane, Japan

[4] The Center for Integrated Kidney Research and Advance (IKRA), Faculty of Medicine, Shimane University, Izumo, Shimane, Japan

[5] Center for Preventive Medicine, Keio University Hospital, Shinjuku-ku, Tokyo, Japan

Published online: 07 October 2025

Graphical Abstract

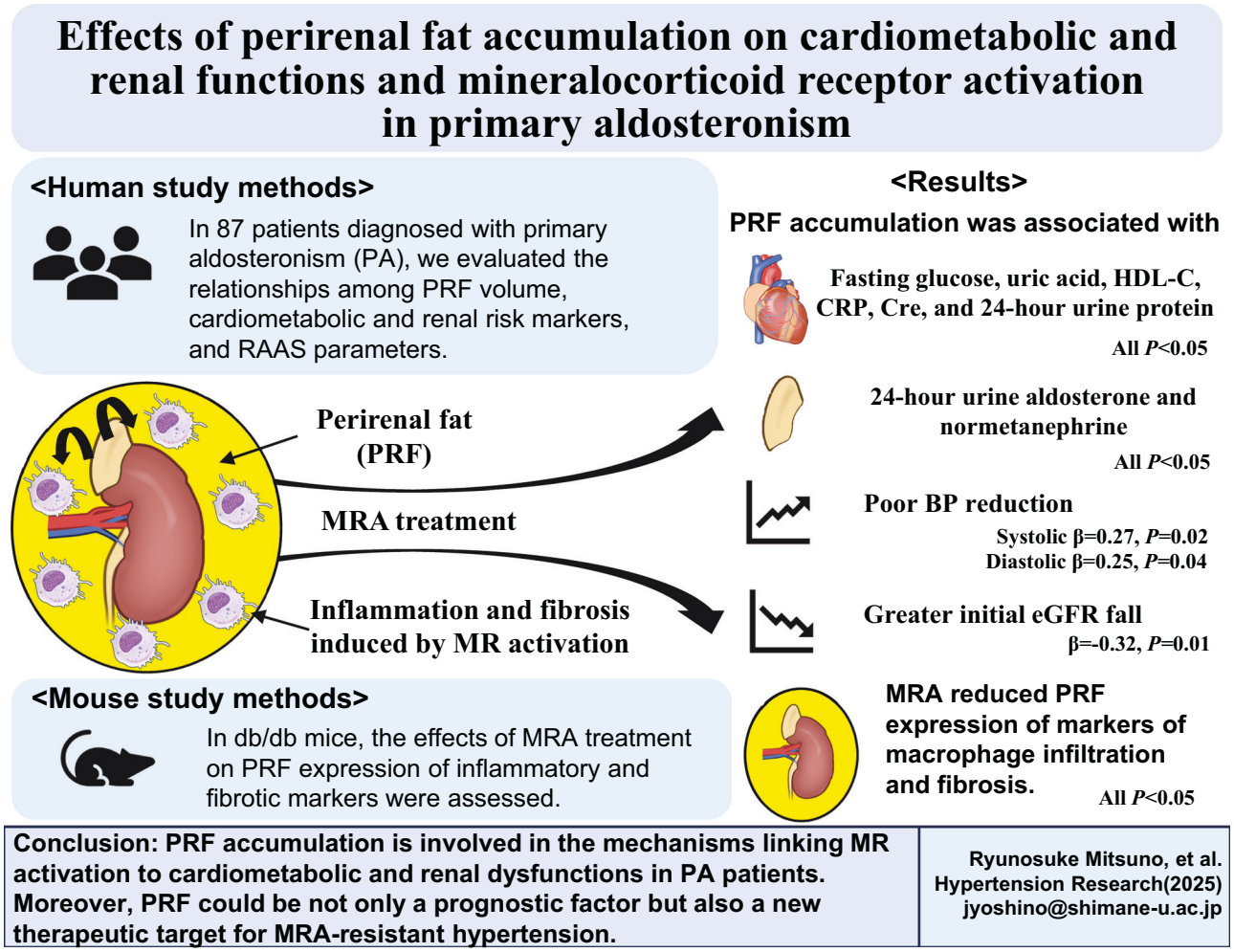

pathogenesis of various cardiometabolic disorders, such as resistant hypertension, arterial stiffness, heart failure, chronic kidney disease (CKD), and metabolic syndrome through the activation of mineralocorticoid receptor (MR) [4–7]. PA is typically curable and treated with adrenalectomy and MR antagonists (MRAs), including steroidal and nonsteroidal agents [3, 8–11]. The mechanisms explaining the relationship between MR activation and cardiometabolic disorders in PA patients remain unclear but could involve dysfunction of adipose tissue, an active metabolic and endocrine organ expressing key renin-angiotensin-aldosterone system (RAAS) regulators including angiotensinogen, angiotensin converting enzyme (ACE), angiotensin II type 1 receptor, aldosterone synthase (CYP11B2), and MR [12–14].

Recent studies have shown that visceral fat (VF) accumulation is associated with increased aldosterone level and cardiac and renal dysfunctions in PA patients [15–17]. In addition, we reported that the volume of renal sinus fat, an ectopic fat depot located at the renal cavity, is associated with cardiometabolic traits and RAAS parameters in PA patients [7]. Perirenal fat (PRF) is another ectopic fat depot localized in the retroperitoneal space surrounding the kidneys and is supported by the renal fascia, filling the space between the kidney and neighboring retroperitoneal tissues, renal parenchyma, and adrenal gland [18]. Previous studies have demonstrated that PRF accumulation is a risk factor for hypertension [19], cardiovascular disease [20], CKD [21], and metabolic syndrome [22]. However, the associations between PRF accumulation and cardiometabolic and renal functions in PA patients are largely unknown. In addition, it remains unclear whether PRF and VF have distinctive roles in the pathophysiology of PA.

The major purpose of the present study was to evaluate the involvement of PRF accumulation in the mechanism linking MR activation to cardiometabolic and renal dysfunctions in patients with PA. To this end, we retrospectively measured PRF volume and VFV by abdominal

CT and evaluated the relationship between PRF volume and clinical parameters in well-phenotyped PA patients. In addition, we determined the effects of MRA administration on cellular and molecular events associated with inflammation and fibrosis, potent downstream targets of MR signaling [23, 24], by analyzing PRF obtained from genetically obese (db/db) mice.

Methods

Study subjects

We conducted a single-center retrospective study at Keio University Hospital in Tokyo and first assessed 335 patients older than 18 years of age who were diagnosed with having PA based on diagnostic tests (i.e., captopril challenge test, furosemide-upright test, or saline infusion test) and those who underwent adrenal venous sampling (AVS) between January 1, 2016 and October 31, 2021. We defined the observation period as the period between the initiation of MRA administration (baseline) and the next outpatient visit (follow-up). To directly evaluate the effects of MRA administration on clinical parameters, we excluded patients who were newly prescribed or changed the dose of other antihypertensive drugs, such as calcium channel blockers ($n = 108$), renin–angiotensin system inhibitors (RASI) ($n = 19$), alpha blockers ($n = 7$), or beta blockers ($n = 1$) during the observation period. In addition, we excluded patients with missing baseline blood pressure (BP) data ($n = 25$), follow-up BP data ($n = 30$), and those without a blood test for plasma aldosterone concentration (PAC) at 7:00 AM ($n = 18$) or an abdominal to pelvic CT scan within 6 months ($n = 30$). We also excluded patients diagnosed with subclinical Cushing's syndrome (SCS) ($n = 6$), Cushing's syndrome (CS) ($n = 2$), and those who had a single kidney after surgery ($n = 2$). As a result, this study included 87 PA patients (Supplementary Fig. 1). This study was approved by the Research Ethics Committee of Keio University School of Medicine (approval number: 20221032) and informed consent was obtained by the opt-out method.

Clinical data and assay methods

Demographic data, such as age, sex, body mass index (BMI), type of antihypertensive agent, and comorbidities, were collected at the initiation of MRA administration (baseline). We also obtained the clinical data at baseline and follow-up periods, such as systolic and diastolic BP, and serum creatinine concentration (mg/dL). Estimated glomerular filtration rate (eGFR) was calculated using GFR estimation formula for the Japanese population [25]. The differences in the systolic and diastolic BP, serum creatinine concentration, and eGFR between baseline and the follow-up after MRA initiation were abbreviated as ΔSBP, ΔDBP, ΔCr and ΔeGFR, respectively; the follow-up values were obtained at the first outpatient visit and at 6–12 months. The BP was measured at our outpatient office with patients seated after a rest. The characteristics of hormone assays used in this study are provided in Supplementary Table 1.

Diagnosis and subtypes of primary aldosteronism

PA was diagnosed according to the guidelines of the Japan Endocrine Society [1] and the Japanese Society of Hypertension [26] as (1) a high aldosterone-to-renin ratio (ARR) (>40 with PAC expressed in pg/mL and ARC expressed in pg/ml) and (2) at least one positive result on a confirmatory test (i.e., captopril challenge test, furosemide-upright test, or saline infusion test).

To determine whether aldosterone overproduction was lateralized in a unilateral adrenal gland, we performed AVS in the PA patients. Of the 87 patients, 22 were diagnosed with unilateral PA and 65 were diagnosed with bilateral PA. The lateralized ratio (LR) was calculated by dividing the ratio of the PAC/serum cortisol concentration (PAC/F) in the ipsilateral adrenal vein by the ratio of PAC/F in the contralateral adrenal vein. The contralateral ratio (CR) was calculated by dividing the ratio of PAC/F in the contralateral adrenal vein by the ratio of PAC/F in the inferior vena cava. Lateralization of overproduction in the adrenal glands was indicated when LR was ≥4 with adrenocorticotropic hormone (ACTH) stimulation and when CR was <1 with ACTH stimulation [27]. In cases where AVS was unsuccessful or difficult, the diagnosis was determined by a medical team that involved multiple experienced endocrinologists.

Perirenal fat volume, visceral fat volume, and subcutaneous fat volume measurements

All subjects underwent multi-slice helical CT with a 1.2-mm slice thickness, starting from the upper edge of the liver to the pelvis within 6 months of the PA diagnosis. All imaging analyses were performed on a dedicated Advantage Workstation (version 3.2, GE Healthcare, Tokyo, Japan) as we previously described [7, 28]. PRF volume (cm^3), VFV (cm^3), and subcutaneous fat volume (SFV, cm^3) were determined by a semi-automated method that required a slice-by-slice manual definition of borders on CT axial images, and each volume was obtained. The PRF area was defined as adipose tissue supported by the renal fascia. The subcutaneous fat area was defined as adipose tissue between the skin and muscle layers. The visceral fat area was defined as adipose tissue located in the abdominal cavity. The fatty tissue was defined between −200 and −40 Hounsfield

units. PRF% was calculated by dividing the PRF volume with VFV.

Animal experimentation

Male leptin receptor deficient C57/BLKS/J db/db and their heterozygous db/+ mice were purchased from the Jackson Laboratory (Bar Harbor, ME, USA). Mice were housed under controlled light (12 h light/12 h dark) and fed a regular-chow diet *ad libitum* with free access to water. To evaluate the effects of MRA administration on PRF biology, mice were treated orally with either finerenone (10 mg/kg-body p.o.) (Bayer Pharma Japan, Osaka, Japan) or vehicle (10% ethanol, 40% Solutol Kolliphor HS15 [#42966; Sigma-Aldrich, St. Louis, MO, USA], and 50% water) ($n = 5$–6) for 10 weeks. The selection of the 10 mg/kg-body dose of finerenone was determined based on previous studies that revealed that this dose regimen effectively treated cardiometabolic and renal dysfunctions [29, 30]. Mice were anesthetized for collecting PRF samples. Plasma aldosterone concentration was determined by using the Aldosterone ELISA Kit (#ADI-900-173; Enzo Life Sciences, Farmingdale, NY, USA). All animal studies were approved by the Institutional Animal Care and Use Committees at Keio University.

RNA isolation and real-time PCR

Total RNA was isolated from frozen PRF samples by using the RNeasy Plus Mini Kit (#74134; Qiagen, Valencia, CA, USA) and Trizol (Invitrogen, Carlsbad, CA, USA). Gene expression was determined using the KAPA SYBR FAST Universal Kit (#KK4602; Sigma-Aldrich, St. Louis, MO, USA) as we previously described [31, 32]. The expression of each gene was determined by normalizing the Ct (cycle threshold) value of each sample to the housekeeping control gene, ribosomal protein (*36b4*). Primer details are listed in Supplementary Table 2. The composite expression levels of genes encoding proteins involved in macrophage (CD68, CD11b, F4/80, MCP-1) and fibrosis (COL1A1, COL3A1, COL6A1, TGF-β1, CTGF, FN) were calculated after expression of each gene to a Z-distribution as we previously described [33].

Histological assessment

For the histological assessments, PRF samples were fixed in paraformaldehyde and embedded in paraffin. After the deparaffinization step, sections were stained with Masson's trichrome for collagen. Immunostaining was performed by using a monoclonal mouse F4/80 antibody (#28463-1-AP, Proteintech, Manchester, United Kingdom). We calculated the percentage of positively stained area (%Area) for F4/80 (brown) and Masson's trichrome (blue) relative to the total area. We randomly selected 3–4 fields per histological section and the mean %Area was reported. In addition, we performed a quantitative analysis of adipocyte size using hematoxylin and eosin–stained sections of PRF. All the images were acquired with Virtual Slide Scanner (Hamamatsu Photonics, Shizuoka, Japan). Image density and area were quantified using ImageJ software (NIH ImageJ 1.54; https://imagej.nih.gov/ij).

Statistical analysis

Data were presented as median (interquartile range) for continuous variables and number and percentage for categorical variables unless otherwise stated. The comparisons between unilateral and bilateral groups were assessed in Mann–Whitney test for continuous variables and Fisher's exact test for proportions. Spearman correlation coefficient (ρ) was calculated to evaluate correlations between PRF% and variables. Partial rank correlation was used to adjust the association between PRF% and 24-h urine aldosterone after accounting for 24-h urine sodium chloride. Multivariate regression analyses were performed to examine correlations between PRF% and the variables of interest. We used the ratio of the prescribed MRA dose to the maximum MRA dose specified in the guideline of the Japan Endocrine Society [1] (eplerenone 100 mg; esaxerenone 5 mg; spironolactone 100 mg) as a variable in the multivariate linear regression analysis. Differences between MRA- and vehicle-treated mice were assessed by using Student's unpaired t-tests. All significance tests were two-tailed, and $P < 0.05$ was considered statistically significant. SPSS (ver. 28; IBM Corp., NY, USA) was used to perform all statistical analyses.

Results

Associations between PRF volume and cardiometabolic and RAAS parameters in PA patients

Baseline characteristics of the 87 PA patients included in this study were summarized in Table 1. As expected, PAC, ARR, 24-h urine aldosterone, serum sodium concentration, prevalence of adrenal nodule, and urine albumin level were significantly higher while ARC and serum potassium concentration were lower in the unilateral PA group than in the bilateral PA group (Table 1). We first evaluated the relationships among PRF accumulation manifested by PRF%, VFV and cardiometabolic, renal, and RAAS parameters. Both PRF% and VFV positively correlated with various cardiometabolic and renal risk markers, such as BMI, serum

Table 1 Baseline characteristics

	Total	Unilateral	Bilateral	*P* value
Number	87	22	65	
Age, years	53 [45, 58]	54 [49, 60]	51 [44, 58]	0.434
Female, *n* (%)	50 (57.5)	10 (45.5)	40 (61.5)	0.218
Height, cm	164.5 [157.9, 170.2]	167.1 [157.3, 169.9]	162.5 [158.0, 171.0]	0.578
Body weight, kg	66.7 [58.7, 77.2]	68.2 [60.4, 77.5]	66.6 [56.8, 76.8]	0.773
BMI, kg/m^2	25.0 [22.2, 27.5]	24.9 [22.0, 27.8]	25.0 [22.2, 27.5]	0.977
PRF, cm^3	188.0 [92.5, 434.0]	188.1 [126.0, 601.0]	188.0 [67.9, 359.8]	0.249
VFV, cm^3	2407 [1715, 3742]	2553 [1898, 4145]	2352 [1656, 3581]	0.418
SFV, cm^3	5958 [4460, 8181]	6182 [4378, 8387]	5854 [4595, 8043]	0.675
PRF%	7.66 [5.37, 12.05]	7.67 [6.32, 14.14]	7.56 [5.24, 11.38]	0.181
VFV/SFV ratio	0.42 [0.28, 0.58]	0.49 [0.29, 0.63]	0.38 [0.27, 0.57]	0.452
Diabetes mellitus, *n* (%)	5 (5.7)	1 (4.5)	4 (6.2)	>0.999
Cardiovascular disease, *n* (%)	0 (0.0)	0 (0.0)	0 (0.0)	>0.999
Antihypertensive medication use, *n* (%)	68 (78.2)	19 (86.4)	49 (75.4)	0.378
Calcium-channel blockers	65 (74.7)	19 (86.4)	46 (70.8)	0.169
Alpha-blockers	5 (5.7)	2 (9.1)	3 (4.6)	0.597
Beta-blockers	2 (2.3)	1 (4.5)	1 (1.5)	0.444
RASI	0 (0.0)	0 (0.0)	0 (0.0)	>0.999
SBP, mmHg	149 [139, 161]	150 [139, 158]	148 [139, 161]	0.977
DBP, mmHg	93 [85, 100]	95 [83,99]	92 [85, 101]	0.635
ARC, pg/mL	2.30 [2.00, 3.10]	2.00 [1.08, 2.30]	2.50 [2.00, 3.30]	0.024
PAC, pg/mL	224.0 [148.5, 278.0]	318.0 [240.8, 384.0]	187.0 [141.0, 253.0]	<0.001
ARR	86.0 [55.1, 149.2]	175.5 [89.4, 252.0]	70.9 [50.4, 120.0]	<0.001
Adrenal nodule, *n* (%)	56 (64.4)	20 (90.9)	36 (55.4)	0.002
Serum cortisol, μg/dL	14.7 [12.3, 16.7]	15.3 [13.2, 17.7]	14.3 [12.3, 16.6]	0.573
Plasma ACTH, pg/mL	25.8 [20.0, 35.7]	28.7 [22.3, 33.0]	24.8 [19.7, 35.9]	0.581
Plasma BNP, pg/mL	17.9 [11.0, 28.2]	18.2 [9.9, 27.1]	17.9 [11.1, 29.0]	>0.999
Serum creatinine, mg/dL	0.72 [0.64, 0.82]	0.74 [0.68, 0.86]	0.72 [0.64, 0.81]	0.461
Serum BUN, mg/dL	12.7 [10.6, 15.8]	12.0 [9.5, 14.6]	13.1 [10.9, 16.1]	0.196
eGFR, mL/min/1.73 m^2	75.0 [67.5, 83.5]	74.0 [68.0, 85.8]	75.0 [66.0, 83.0]	0.777
Serum Na, mmol/L	141.3 [140.3, 142.6]	142.1 [141.2, 143.5]	140.9 [140.2, 142.4]	0.017
Serum K, mmol/L	3.80 [3.60, 4.10]	3.55 [3.10, 3.77]	3.90 [3.70, 4.10]	<0.001
Urine albumin, mg/gCr	7.85 [4.70, 16.88]	15.70 [7.23, 36.77]	6.55 [4.25, 10.70]	0.002
24-h urine protein, mg/day	0.00 [0.00, 83.00]	104.00 [0.00, 131.50]	0.00 [0.00, 67.25]	0.051
Serum uric acid, mg/dL	5.10 [4.70, 6.20]	5.80 [5.05, 6.68]	5.00 [4.40, 5.90]	0.099
Serum TG, mg/dL	93.0 [64.5, 137.5]	134.0 [91.0, 165.5]	92.0 [53.0, 120.0]	0.082
Serum LDL-C, mg/dL	118.0 [102.0, 137.0]	132.0 [108.5, 140.0]	117.5 [102.0, 132.5]	0.398

Table 1 (continued)

	Total	Unilateral	Bilateral	*P* value
Serum HDL-C, mg/dL	56.0 [49.0, 69.3]	57.5 [43.3, 67.5]	56.0 [49.8, 70.8]	0.570
TGs/HDL-C ratio	1.79 [0.88, 2.60]	2.42 [1.18, 3.55]	1.54 [0.84, 2.51]	0.090
Fasting plasma glucose, mg/dL	101.0 [96.0, 106.0]	101.5 [97.0, 105.5]	100.0 [95.0, 106.5]	0.610
HbA1c, %	5.50 [5.30, 5.70]	5.40 [5.20, 5.65]	5.60 [5.35, 5.70]	0.050
Serum C-reactive protein, mg/dL	0.03 [0.01, 0.06]	0.04 [0.02, 0.14]	0.03 [0.01, 0.06]	0.320
24-h urine sodium chloride, g/day	7.50 [5.50, 9.90]	8.58 [5.95, 11.32]	7.27 [5.35, 8.95]	0.198
24-h urine aldosterone, μg/day	11.6 [8.8, 17.1]	17.3 [13.1, 25.1]	10.0 [8.3, 13.4]	<0.001
24-h urine metanephrine, mg/day	0.10 [0.09, 0.13]	0.10 [0.09, 0.14]	0.11 [0.09, 0.13]	0.504
24-h urine normetanephrine, mg/day	0.22 [0.17, 0.26]	0.24 [0.19, 0.26]	0.22 [0.17, 0.27]	0.400
24-h urine total metanephrines, mg/day	0.32 [0.27, 0.39]	0.33 [0.30, 0.39]	0.32 [0.27, 0.40]	0.662

Data were presented as median [interquartile range (IQR)] for continuous variables and number and percentage for categorical variables

BMI body mass index, *VFV* visceral fat volume, *SFV* subcutaneous fat volume, *RASI* renin–angiotensin system inhibitors, *SBP* systolic blood pressure, *DBP* diastolic blood pressure, *ARC* active renin concentration, *PAC* plasma aldosterone concentration, *ARR* aldosterone-to-renin ratio, *ACTH* adrenocorticotropic hormone, *BNP* brain natriuretic peptide, *eGFR* estimated glomerular filtration rate, *TG* triglycerides, *LDL-C* low density lipoprotein cholesterol, *HDL-C* high density lipoprotein cholesterol, *HbA1c* glycated hemoglobin A1c

creatinine concentration, serum uric acid concentration, serum triglyceride (TG) concentration, TG/high-density lipoprotein cholesterol (HDL-C) ratio [34], fasting glucose concentration, and serum C-reactive protein (CRP) concentration, while it negatively correlated with serum HDL-C concentration in PA patients (all $P < 0.05$) (Table 2, and Supplementary Table 3). In addition, PRF% was positively correlated with 24-h urine aldosterone level, 24-h urine normetanephrine level, and 24-h urine total metanephrines level ($P < 0.05$) (Table 2). Furthermore, partial rank correlation showed the significant association between PRF% and 24-h urine aldosterone after adjusting for 24-h urine sodium chloride ($P = 0.03$). In contrast, while VFV was positively associated with 24-h urine normetanephrine and total metanephrines levels ($P < 0.05$), it did not correlate with 24-h urine aldosterone level (Supplementary Table 3). We found overall similarity in associations among these parameters between the unilateral and bilateral PA groups (Table 2). These findings lead us to hypothesize that PRF may be more closely linked to systemic MR activation than VFV. We therefore extended our investigation to a longitudinal cohort study and evaluated the effect of PRF accumulation on MR activation and BP and renal outcomes.

Associations between PRF volume and therapeutic response to MRA treatment

We next determined whether PRF accumulation is involved in therapeutic response following MRA treatment in PA patients. The observation period between baseline and the first outpatient follow-up was 3 [2–4] weeks. Seventy patients received eplerenone (12.5–100 mg/day), fifteen received esaxerenone (2.5–5 mg/day), and two received spironolactone (25 mg/day) (Supplementary Table 4). Intriguingly, PRF%, but not VFV, positively correlated with ΔSBP and ΔDBP, while it negatively correlated with ΔeGFR (all $P < 0.05$) (Fig. 1 and Supplementary Fig. 2). After adjusting for potential confounders such as age, sex, BMI, baseline values, 24-h urine sodium chloride level, subtype of PA, antihypertensive medication use, and MRA dose, PRF% remained positively correlated with ΔSBP, ΔDBP, and ΔCr, and negatively correlated with ΔeGFR (all $P < 0.05$) (Table 3). PRF% was similarly associated with ΔCr (unilateral group, $\rho = 0.42$, $P = 0.06$; bilateral group, $\rho = 0.37$, $P < 0.01$) and ΔeGFR (unilateral group, $\rho = -0.31$, $P = 0.17$; bilateral group, $\rho = -0.34$, $P < 0.01$) after MRA initiation in both PA subtypes. However, the association between PRF% and poor reduction of blood pressure at the initial outpatient visit was evident in the bilateral group (systolic, $\rho = 0.44$, $P < 0.01$; diastolic, $\rho = 0.39$, $P < 0.01$) but not in the unilateral group (systolic, $\rho = 0.04$, $P = 0.87$; diastolic, $\rho = -0.01$, $P = 0.96$), indicating the difference between PA subtypes in the antihypertensive response to MRA treatment. Consistently, PRF% positively correlated with ΔCr, while it negatively correlated with ΔeGFR (all $P < 0.05$) at 6–12 months after MRA initiation (Supplementary Fig. 3). Although there was no association between PRF% and changes in BP (Supplementary Fig. 3), PRF% positively correlated with the number of antihypertensive medications required to control BP at 6–12 months after MRA initiation ($\rho = 0.27$, $P = 0.03$). In addition, despite the relatively small number of patients who underwent surgery ($n = 18$), the overall trends were similar with those observed in the MRA-treated

Table 2 Associations between PRF% and cardiometabolic and renal risk markers and renin-angiotensin-aldosterone system (RAAS) parameters in PA patients

	Total		Unilateral		Bilateral	
	ρ	*P*	ρ	*P*	ρ	*P*
Age, years	0.09	0.412	−0.04	0.845	0.14	0.283
BMI, kg/m^2	0.40	<0.001	0.45	0.035	0.37	0.002
VFV, cm^3	0.61	<0.001	0.80	<0.001	0.54	<0.001
SFV, cm^3	0.10	0.370	0.09	0.706	0.07	0.590
VFV/SFV ratio	0.71	<0.001	0.86	<0.001	0.65	<0.001
SBP, mmHg	−0.04	0.684	0.31	0.155	−0.15	0.221
DBP, mmHg	−0.11	0.293	0.29	0.186	−0.26	0.036
ARC, pg/mL	−0.09	0.417	0.35	0.107	−0.20	0.114
PAC, pg/mL	0.00	0.975	−0.04	0.859	−0.09	0.462
ARR	0.12	0.290	−0.23	0.294	0.11	0.395
Serum creatinine, mg/dL	0.40	<0.001	0.62	0.002	0.32	0.009
Serum BUN, mg/dL	0.00	0.999	0.10	0.647	−0.02	0.855
eGFR, mL/min/1.73 m^2	0.08	0.467	−0.04	0.857	0.11	0.405
Serum Na, mmol/L	0.15	0.164	0.16	0.476	0.15	0.226
Serum K, mmol/L	−0.09	0.411	−0.01	0.980	−0.06	0.644
24-h urine protein, mg/day	0.23	0.082	0.23	0.408	0.20	0.169
Serum uric acid, mg/dL	0.55	<0.001	0.38	0.153	0.64	<0.001
Serum TG, mg/dL	0.41	0.007	0.25	0.467	0.47	0.006
Serum LDL-C, mg/dL	−0.19	0.088	−0.41	0.080	−0.14	0.257
Serum HDL-C, mg/dL	−0.49	<0.001	−0.45	0.049	−0.53	<0.001
TGs/HDL-C ratio	0.42	0.005	0.20	0.555	0.51	0.003
Fasting plasma glucose, mg/dL	0.25	0.021	0.48	0.024	0.18	0.165
HbA1c, %	0.14	0.201	0.13	0.571	0.21	0.098
Serum C-reactive protein, mg/dL	0.25	0.047	0.62	0.003	0.02	0.910
24-h urine sodium chloride, g/day	0.15	0.161	0.44	0.043	0.03	0.845
24-h urine aldosterone, μg/day	0.24	0.029	0.21	0.347	0.19	0.135
24-h urine metanephrine, mg/day	0.11	0.381	0.27	0.269	0.11	0.454
24-h urine normetanephrine, mg/day	0.28	0.019	0.52	0.022	0.26	0.073
24-h urine total metanephrines, mg/day	0.28	0.022	0.41	0.081	0.26	0.067

Spearman correlation coefficient (ρ) was calculated to evaluate correlations between PRF% and cardiometabolic and RAAS parameters in PA patients

BMI body mass index, *VFV* visceral fat volume, *SFV* subcutaneous fat volume, *SBP* systolic blood pressure, *DBP* diastolic blood pressure, *ARC* Active renin concentration, *PAC* plasma aldosterone concentration, *ARR* aldosterone-to-renin ratio, *eGFR* estimated glomerular filtration rate, *TG* triglycerides, *LDL-C* low density lipoprotein cholesterol, *HDL-C* high density lipoprotein cholesterol, *HbA1c* glycated hemoglobin A1c

group (Supplementary Fig. 4). Specifically, PRF% tended to be positively correlated with a higher number of antihypertensive medications during the follow-up period, in the adrenalectomy group ($\rho = 0.44$, $P = 0.06$), indicating that PRF may contribute to persistent blood pressure burden regardless of treatment modality.

Effect of oral MRA administration on PRF inflammation and fibrosis in obese mice

Data obtained from studies conducted in rodents suggest that PRF could directly deteriorate renal function through mechanical compression and local secretion of pro-inflammatory cytokines and chemokines [35]. In addition, it was recently reported that hyperaldosteronism is associated with increased expression of selected markers of inflammation and fibrosis in human PRF [36]. Thus, we specifically aimed to evaluate the effects of MR inhibition on selected markers of inflammation and fibrosis, downstream targets of MRA in key metabolic organs such as kidney and heart [37, 38]. To this end, we selected db/db mice that have key phenotypes associated with MR activation, particularly adipose tissue inflammation and fibrosis. We first confirmed db/db mice had increases in plasma aldosterone concentration and expression of monocyte chemoattractant protein-1(MCP-1), a key regulator of

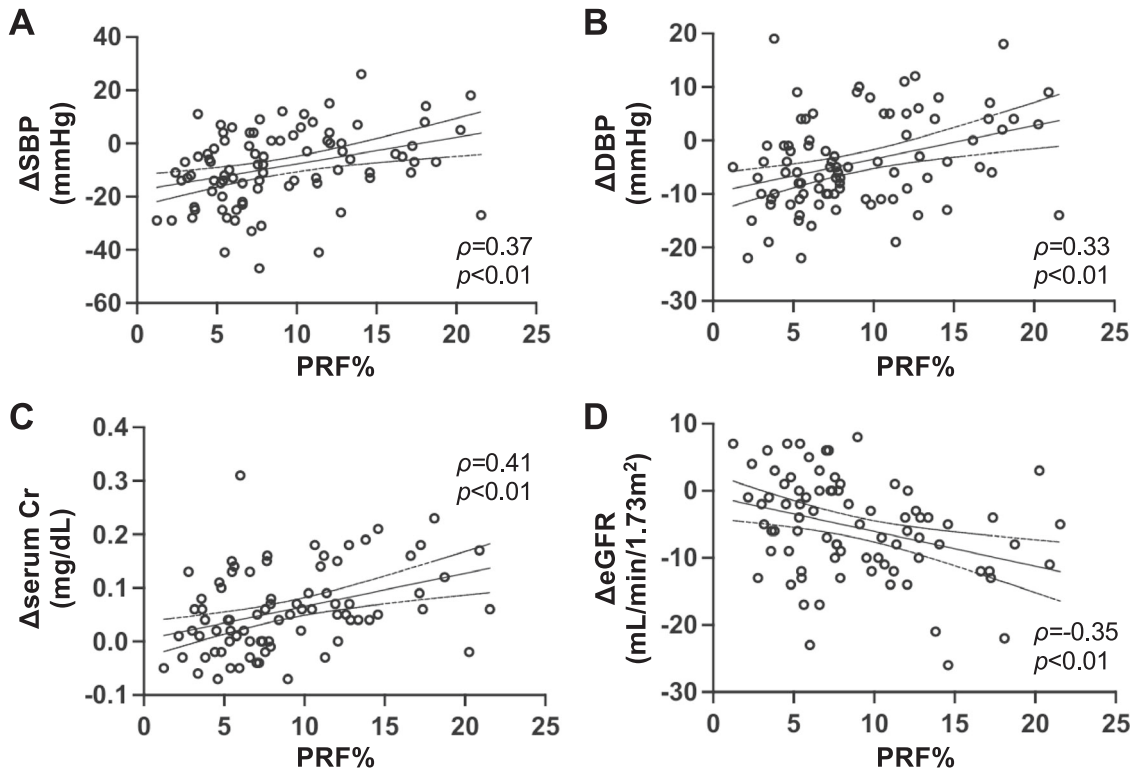

Fig. 1 Associations between PRF% and responses to MRA treatment in PA patients. The differences in the systolic and diastolic BP, creatinine, and eGFR before and after MRA treatment were evaluated and abbreviated as ΔSBP, ΔDBP, ΔCr and ΔeGFR, respectively. We investigated the relationships between perirenal fat (PRF) volume normalized by visceral fat volume (PRF%) and ΔSBP (**A**), Δ DBP (**B**), ΔCr (**C**), and ΔeGFR (**D**). Spearman correlation coefficient (ρ) and *P* value (p) were provided in each plot

macrophage recruitment, and collagen type III alpha 1 chain (COL3A1) in PRF (Supplementary Fig. 5A, B). Intriguingly, oral MRA administration significantly decreased PRF gene expression of MCP-1 and COL3A1 in db/db mice (all $P < 0.05$) (Fig. 2A). In addition, the composite expression values of genes encoding key surrogate markers of macrophage (CD68, CD11b, F4/80, MCP-1) and fibrosis (COL1A1, COL3A1, COL6A1, TGF-β1, CTGF, FN) were significantly downregulated in db/db mice treated with MRA (all $P < 0.05$) (Fig. 2B). Consistent with gene expression data, interstitial macrophage infiltration and fibrosis in PRF, evaluated by F4/80 positive cells and Masson's trichrome collagen staining respectively, were also significantly decreased in db/db mice after oral MRA administration (all $P < 0.05$) (Fig. 2C, D). We found no difference in PRF adipocyte size between control and MRA-treated mice (Supplementary Fig. 5C).

Discussion

We found that both PRF and VF were associated with various cardiometabolic and renal parameters, such as BMI, creatinine, uric acid, TG, fasting glucose, CRP, HDL-C, and TG/HDL-C ratio in PA patients. Our results are consistent with previous studies that found that PRF and visceral fat accumulation are associated with cardiometabolic risk factors in patients with obesity, type 2 diabetes, and CKD [39–41]. In addition, PRF volume, but not VFV, positively correlated with 24-h urine aldosterone level, a key RAAS parameter and a risk factor for cardiovascular dysfunction in PA patients [42, 43], suggesting that VFV and PRF may have distinctive roles in the pathophysiology of PA. The complex relationships among PRF accumulation, MR activation, and cardiometabolic and renal dysfunction in PA patients could be explained by several mechanisms. First, PRF accumulation could lead to increased systemic and renal RAAS activity through physical compression of the renal vasculature and nerve system [35]. Second, data obtained from studies conducted in rodents and cultured adipocytes have suggested that aldosterone-induced MR activation induces production of pro-inflammatory cytokines, such as MCP-1 and interleukin-6 (IL-6), in adipocytes [44–46]. Thus, hyperaldosteronism could induce local and systemic inflammation, contributing to the development of cardiometabolic dysfunction. Third, adipocytes have the endogenous capacity to produce aldosterone and PRF-derived aldosterone could cause pro-inflammatory and pro-fibrotic responses in vascular endothelial cells [14]. Taken together, these findings indicate the potential importance of

Table 3 Multivariable regression models exploring the associations between PRF% and ΔSBP, ΔDBP, ΔCr, and ΔeGFR in PA patients

	Model 1			Model 2			Model 3		
	β	95% CI	*P*	*β*	95% CI	*P*	*β*	95% CI	*P*
ΔSBP, mmHg	0.28	0.17–0.39	0.015	0.28	0.16–0.39	0.017	0.27	0.16–0.39	0.022
ΔDBP, mmHg	0.29	0.17–0.41	0.016	0.29	0.17–0.41	0.018	0.25	0.13–0.37	0.040
ΔCr, mg/dL	0.38	0.26–0.51	0.006	0.39	0.26–0.52	0.005	0.32	0.20–0.45	0.018
ΔeGFR, mL/min/1.73m^2	−0.37	−0.50 to −0.24	0.006	−0.37	−0.50 to −0.24	0.005	−0.32	−0.45 to −0.19	0.015

Model 1 adjusted for age, sex, body mass index, and the baseline value of each dependent variable

Model 2 adjusted for age, sex, body mass index, the baseline value of each dependent variable, and 24-h urine sodium chloride. In analyses for ΔSBP and ΔDBP, baseline eGFR was added as an independent variable

Model 3 adjusted for age, sex, body mass index, the baseline value of each dependent variable, 24-h urine sodium chloride, subtype, antihypertensive medication use, and mineralocorticoid receptor antagonist dose. In analyses for ΔSBP and ΔDBP, baseline eGFR was added as an independent variable

The differences in the systolic and diastolic BP, serum creatinine concentration, and eGFR before and after MRA treatment were abbreviated as ΔSBP, ΔDBP, ΔCr and ΔeGFR, respectively

β adjusted β coefficient, *CI* confidence interval

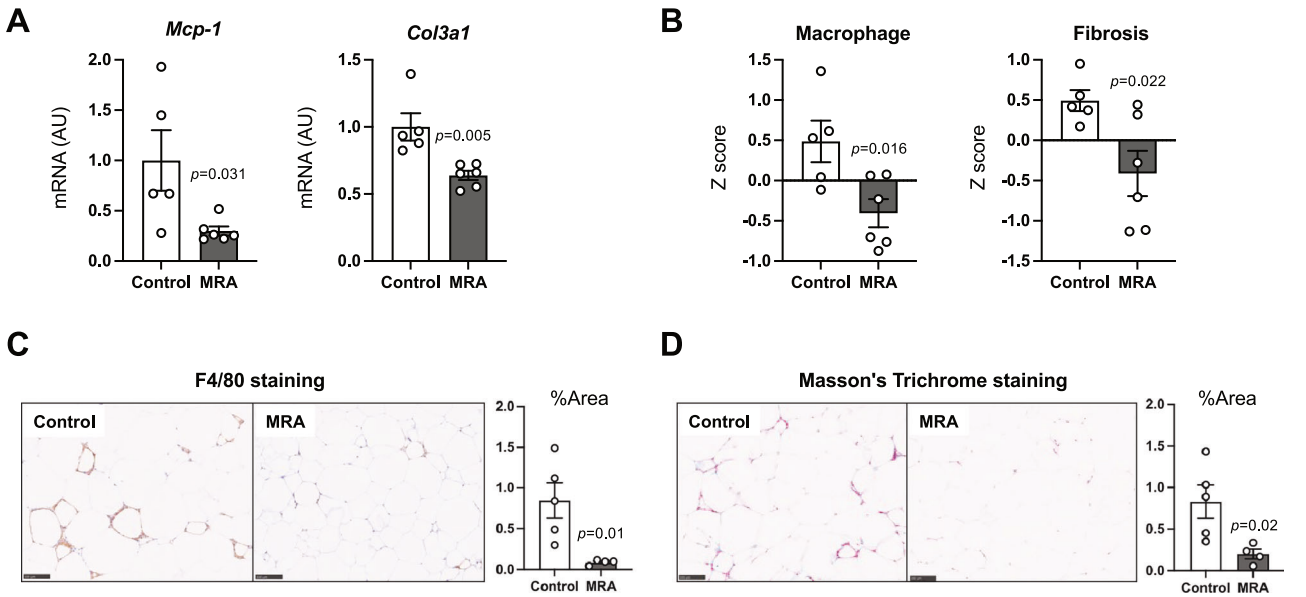

Fig. 2 Effects of oral MRA administration on PRF inflammation and fibrosis in db/db mice. **A** Gene expression of *Mcp-1* and *Col3a1* in PRF obtained from db/db mice treated with MRA or vehicle ($n = 5$–6 per group). **B** The composite expression values of genes encoding key surrogate markers of macrophage (CD68, CD11b, F4/80, MCP-1) and fibrosis (COL1A1, COL3A1, COL6A1, TGF-β1, CTGF, FN) were calculated after expression of each gene to a Z-distribution in db/db mice treated with MRA or vehicle ($n = 5$–6 per group). Interstitial macrophage infiltration and fibrosis in PRF were evaluated by F4/80 positive cells (**C**) and Masson's trichrome collagen staining (**D**). Values are means ± SE. Data were analyzed by Student's unpaired *t* test. *P* value (p) is provided in each figure. *Mcp-1*, monocyte chemoattractant protein-1; *Col3a1*, collagen, type III, *Cd68*, cluster of differentiation 68; *Cd11b (Itgam)*, integrin alpha M; *F4/80 (Adgre1)*, adhesion G protein coupled receptor E1; *Col1a1*, collagen, type I, alpha 1 chain; *Col6a1*, collagen, type VI, alpha 1 chain; *Tgf-β1*, transforming growth factor beta 1; *Ctgf*, connective tissue growth factor

PRF in MR activation and subsequent cardiometabolic and renal dysfunction in PA patients.

MRAs are powerful antihypertensive agents and widely used in patients with resistant hypertension, particularly those with obesity [47] and high salt-sensitivity [48]. Intriguingly, our results suggest that PRF volume, but not VFV, is an independent risk factor for poor therapeutic response of BP to MRA treatment in PA patients, indicating again that PRF and VFV may have distinctive therapeutic roles. To our knowledge, this is the first report showing the

relationships among PRF accumulation, RAAS parameters, and MRA treatment in PA patients. The mechanisms between PRF accumulation and poor response to MRA treatment remain unclear but could be explained by RAAS-independent BP-regulating mechanisms such as renal sympathetic nerve activity. Supporting this notion, we identified the positive relationship between PRF volume and 24-h level of urine total metanephrine, a key indicator of systemic sympathetic activity involved in hypertension and other cardiometabolic abnormalities [49–51]. According to the comprehensive analyses of catecholamine metabolism, approximately 77% of normetanephrine is derived from sympathetic nerve terminals, whereas about 90% of metanephrine originates from adrenal-medullary chromaffin cells [52]. These findings suggest that the observed positive correlation between PRF% and 24-h urinary normetanephrine likely reflects increased sympathetic activity, although we cannot rule out the possibility that adrenal-medullary output also could be involved in the mechanism explaining the relationship between PRF% and 24-h urine norepinephrine and total metanephrines. Intriguingly, recent studies demonstrate that afferent nerves localized in PRF are major pathogenic drivers of sympathetic nerve activation and abnormally high BP in spontaneous hypertensive rats and removal of PRF or denervation leads to marked and prolonged reduction in sympathetic nerve activity and BP [53]. Indeed, a multicenter, randomized, sham-control trial is currently being conducted to determine whether focused power ultrasound-mediated PRF modification could reduce high BP in patients with primary hypertension [54]. Taken together, these findings suggest that PRF could be not only a novel prognostic factor but also a new therapeutic target for MRA-resistant hypertension in patients with PA.

Another important finding was that PRF volume was positively correlated with the degree of the initial eGFR fall following MRA treatment even after adjustment for potential confounders. Consistently, previous studies have demonstrated acute eGFR fall after PA-specific therapy, such as MRA treatment and adrenalectomy, in PA patients [55–57]. The MRA-induced eGFR fall is likely due to the decrease in glomerular hyperfiltration caused by excess aldosterone [58]. Indeed, we found that PRF volume was positively associated with baseline 24-h urine aldosterone level, a pooled index of aldosterone release. In addition, PRF-derived aldosterone could locally contribute to the development of renal vascular dysfunction, proteinuria, and hyperfiltration [6]. Taken together, these findings lead us to speculate that MRA treatment could induce a profound reduction in glomerular hyperfiltration and acute eGFR fall particularly in patients with excess PRF. However, the effect of the initial eGFR fall on long-term prognosis in PA patients remains unclear because of inconsistent results from previous studies that found the degree of initial eGFR fall was associated with favorable or unfavorable cardiovascular and renal outcomes [55–57]. The discrepancy among these studies could be related to differences in subject characteristics (e.g., age, race, baseline kidney function), type of MRA, and post-treatment observation period. Additional studies are required to understand the complex relationships among PRF accumulation, MRA-induced initial eGFR fall, and long-term outcome in PA patients.

In the present study, we found MRA treatment markedly decreased expression of selected markers of macrophage infiltration and fibrosis in obese mice, which appears to be consistent with data obtained from the studies conducted in type 1 diabetic rat model [59]. As discussed above, excess aldosterone could cause monocyte and macrophage infiltration and pro-inflammatory and pro-fibrotic changes through the MR activation [46]. Data obtained from the studies conducted in myeloid MR knockout mice suggest that MR activation is involved in regulating MCP-1 gene expression and macrophage inflammatory responses through modulation of the serum-and-glucocorticoid-inducible-kinase-1 (SGK1)/nuclear factor-κB (NF-κB) signaling pathway [60, 61]. It is therefore possible that MRA treatment could suppress SGK1/NF-κB-mediated inflammatory program of residual macrophages in PRF. Additional studies are needed to further determine the precise molecular mechanism linking the MR activation to macrophage infiltration in PRF. Consistent with these experimental findings, it was recently reported that patients with aldosterone-producing adenoma had increased gene expression of selected markers of inflammation and fibrosis in adipose tissue [36]. PRF inflammation may directly affect the function of adjacent organs including blood vessels and kidney via paracrine secretion of pro-inflammatory cytokines and adipokines [35]. In addition, excess PRF fibrosis may cause harmful impact on physical compression of renal structures. Taken together, these findings suggest that MRA-induced renal benefits could be mediated, at least in part, by the resolution of inflammation and fibrosis in PRF. However, caution is warranted when extrapolating data obtained from the studies conducted in db/db mice to patients with PA, because the two models differ markedly in their BP profiles.

One of the limitations of our study was that we were unable to determine the causal relationships among the key parameters because of the nature of the observational clinical study. We investigated PA patients at a single center, which might have generated selection bias and thus potentially limit the generalizability of our findings. In addition, the effect of long-term MRA treatment on PRF volume remains unexplored. Indeed, it was recently reported that cardio and renoprotective agents, such as liraglutide and dapagliflozin, and weight loss reduce PRF thickness in

people with obesity and/or type 2 diabetes [62–64]. Therefore, additional studies are needed to determine whether MR antagonist decreases PRF volume and whether PRF reduction is associated with cardiometabolic benefits-induced by MRA. Finally, although we specifically aimed to evaluate the effect of MRA administration on PRF inflammation and fibrosis in obese-diabetes mouse model (db/db) that have key phenotypes associated with MR activation, particularly increased plasma aldosterone concentration and adipose tissue inflammation and fibrosis [23, 24], we are aware that db/db mice may not be an ideal mouse model of PA. In addition, the effects of MRA administration on PRF biology in lean mice remain unexplored.

In conclusion, the results from the present study suggest that PRF accumulation is involved in the mechanisms linking MR activation to cardiometabolic and renal dysfunctions in PA patients. Our study also indicates that PRF and VF may have distinctive roles in the pathogenesis of PA and therapeutic response to MRA treatment. Additional studies are needed to determine whether PRF volume is associated with long-term prognosis after MRA treatment and understand precise action mechanisms of MRA in PRF by analyzing different mouse models and cell culture systems.

Acknowledgements The authors are grateful to the study participants for their participation. We also thank members in the Yoshino lab for critical discussions and suggestions.

Compliance with ethical standards

Conflict of interest The authors declare no competing interests.

References

1. Naruse M, Katabami T, Shibata H, Sone M, Takahashi K, Tanabe A, et al. Japan Endocrine Society clinical practice guideline for the diagnosis and management of primary aldosteronism 2021. Endocr J. 2022;69:327–59.
2. Funder JW, Carey RM, Mantero F, Murad MH, Reincke M, Shibata H, et al. The management of primary aldosteronism: case detection, diagnosis, and treatment: an endocrine society clinical practice guideline. J Clin Endocrinol Metab. 2016;101:1889–916.
3. Yoshida Y, Shibata H. Recent progress in the diagnosis and treatment of primary aldosteronism. Hypertens Res. 2023;46:1738–44.
4. Huby AC, Antonova G, Groenendyk J, Gomez-Sanchez CE, Bollag WB, Filosa JA, et al. Adipocyte-derived hormone leptin is a direct regulator of aldosterone secretion, which promotes endothelial dysfunction and cardiac fibrosis. Circulation. 2015;132:2134–45.
5. Schinner S, Willenberg HS, Krause D, Schott M, Lamounier-Zepter V, Krug AW, et al. Adipocyte-derived products induce the transcription of the StAR promoter and stimulate aldosterone and cortisol secretion from adrenocortical cells through the Wnt-signaling pathway. Int J Obes. 2007;31:864–70.
6. Briones AM, Nguyen Dinh Cat A, Callera GE, Yogi A, Burger D, He Y, et al. Adipocytes produce aldosterone through calcineurin-dependent signaling pathways: implications in diabetes mellitus-associated obesity and vascular dysfunction. Hypertension. 2012;59:1069–78.
7. Mitsuno R, Kaneko K, Nakamura T, Kojima D, Mizutani Y, Azegami T, et al. Association between renal sinus fat and cardiometabolic and renin-angiotensin system parameters in primary aldosteronism. J Endocr Soc. 2023;8:bvad154.
8. Yoshida Y, Shibata H. Evolution of mineralocorticoid receptor antagonists, aldosterone synthase inhibitors, and alternative treatments for managing primary aldosteronism. Hypertens Res. 2025;48:854–61.
9. Matsuda N, Yoshida Y, Inobe N, Yoshimura M, Iwamoto M, Nagai S, et al. Antihypertensive effects and changes in extracellular water content by mineralocorticoid receptor antagonists in patients with primary aldosteronism. Hypertens Res. 2025;48:553–62.
10. Shibata H. Adrenal ablation therapy for unilateral primary aldosteronism: pros and cons. Hypertens Res. 2023;46:787–9.
11. Yoshida Y, Yoshida R, Shibuta K, Ozeki Y, Okamoto M, Gotoh K, et al. Quality of life of primary aldosteronism patients by mineralocorticoid receptor antagonists. J Endocr Soc. 2021;5:bvab020.
12. Engeli S, Gorzelniak K, Kreutz R, Runkel N, Distler A, Sharma AM. Co-expression of renin-angiotensin system genes in human adipose tissue. J Hypertens. 1999;17:555–60.
13. Schling P, Mallow H, Trindl A, Loffler G. Evidence for a local renin angiotensin system in primary cultured human preadipocytes. Int J Obes Relat Metab Disord. 1999;23:336–41.
14. Nguyen Dinh Cat A, Briones AM, Callera GE, Yogi A, He Y, Montezano AC, et al. Adipocyte-derived factors regulate vascular smooth muscle cells through mineralocorticoid and glucocorticoid receptors. Hypertension. 2011;58:479–88.
15. Haze T, Ozawa M, Kawano R, Haruna A, Ohki Y, Suzuki S, et al. Effect of the interaction between the visceral-to-subcutaneous fat ratio and aldosterone on cardiac function in patients with primary aldosteronism. Hypertens Res. 2023;46:1132–44.
16. Haze T, Hatakeyama M, Komiya S, Kawano R, Ohki Y, Suzuki S, et al. Association of the ratio of visceral-to-subcutaneous fat volume with renal function among patients with primary aldosteronism. Hypertens Res. 2021;44:1341–51.
17. Shibayama Y, Wada N, Baba S, Miyano Y, Obara S, Iwasaki R, et al. Relationship between visceral fat and plasma aldosterone concentration in patients with primary aldosteronism. J Endocr Soc. 2018;2:1236–45.
18. Liu BX, Sun W, Kong XQ. Perirenal fat: a unique fat pad and potential target for cardiovascular disease. Angiology. 2019;70:584–93.
19. Ricci MA, Scavizzi M, Ministrini S, De Vuono S, Pucci G, Lupattelli G. Morbid obesity and hypertension: the role of perirenal fat. J Clin Hypertens. 2018;20:1430–7.
20. Huang N, Mao EW, Hou NN, Liu YP, Han F, Sun XD. Novel insight into perirenal adipose tissue: a neglected adipose depot linking cardiovascular and chronic kidney disease. World J Diabetes. 2020;11:115–25.
21. Geraci G, Zammuto MM, Mattina A, Zanoli L, Geraci C, Granata A, et al. Para-perirenal distribution of body fat is associated with reduced glomerular filtration rate regardless of other indices of adiposity in hypertensive patients. J Clin Hypertens. 2018;20:1438–46.
22. Guo XL, Tu M, Chen Y, Wang W. Perirenal fat thickness: a surrogate marker for metabolic syndrome in chinese newly diagnosed type 2 Diabetes. Front Endocrinol. 2022;13:850334.
23. Hirata A, Maeda N, Hiuge A, Hibuse T, Fujita K, Okada T, et al. Blockade of mineralocorticoid receptor reverses adipocyte dysfunction and insulin resistance in obese mice. Cardiovasc Res. 2009;84:164–72.
24. Urbanet R, Nguyen Dinh Cat A, Feraco A, Venteclef N, El Mogrhabi S, Sierra-Ramos C, et al. Adipocyte mineralocorticoid

receptor activation leads to metabolic syndrome and induction of prostaglandin D2 synthase. Hypertension. 2015;66:149–57.
25. Matsuo S, Imai E, Horio M, Yasuda Y, Tomita K, Nitta K, et al. Revised equations for estimated GFR from serum creatinine in Japan. Am J Kidney Dis. 2009;53:982–92.
26. Umemura S, Arima H, Arima S, Asayama K, Dohi Y, Hirooka Y, et al. The Japanese Society of Hypertension Guidelines for the Management of Hypertension (JSH 2019). Hypertens Res. 2019;42:1235–481.
27. Kempers MJ, Lenders JW, van Outheusden L, van der Wilt GJ, Schultze Kool LJ, Hermus AR, et al. Systematic review: diagnostic procedures to differentiate unilateral from bilateral adrenal abnormality in primary aldosteronism. Ann Intern Med. 2009;151:329–37.
28. Kaneko K, Mitsuno R, Kojima D, Azegami T, Kosugi S, Nakamura T, et al. Renal sinus fat is associated with intrarenal hemodynamic abnormalities independent of visceral fat in patients with chronic kidney disease. Obes Res Clin Pract. 2024;18:118–23.
29. Droebner K, Pavkovic M, Grundmann M, Hartmann E, Goea L, Nordlohne J, et al. Direct blood pressure-independent anti-fibrotic effects by the selective nonsteroidal mineralocorticoid receptor antagonist finerenone in progressive models of kidney fibrosis. Am J Nephrol. 2021;52:588–601.
30. Gonzalez-Blazquez R, Somoza B, Gil-Ortega M, Martin Ramos M, Ramiro-Cortijo D, Vega-Martin E, et al. Finerenone attenuates endothelial dysfunction and albuminuria in a chronic kidney disease model by a reduction in oxidative stress. Front Pharm. 2018;9:1131.
31. Yoshino M, Yoshino J, Kayser BD, Patti GJ, Franczyk MP, Mills KF, et al. Nicotinamide mononucleotide increases muscle insulin sensitivity in prediabetic women. Science. 2021;372:1224–9.
32. Yamaguchi S, Franczyk MP, Chondronikola M, Qi N, Gunawardana SC, Stromsdorfer KL, et al. Adipose tissue NAD(+) biosynthesis is required for regulating adaptive thermogenesis and whole-body energy homeostasis in mice. Proc Natl Acad Sci USA. 2019;116:23822–8.
33. Qi N, Franczyk MP, Yamaguchi S, Kojima D, Hayashi K, Satoh A, et al. Adipocyte-specific inactivation of NAMPT, a key NAD(+) biosynthetic enzyme, causes a metabolically-unhealthy lean phenotype in female mice during aging. Am J Physiol Endocrinol Metab. 2024;(e-pub ahead of print 20240529;https://doi.org/10.1152/ajpendo.00313.2023.
34. McLaughlin T, Reaven G, Abbasi F, Lamendola C, Saad M, Waters D, et al. Is there a simple way to identify insulin-resistant individuals at increased risk of cardiovascular disease? Am J Cardiol. 2005;96:399–404.
35. Hammoud SH, AlZaim I, Al-Dhaheri Y, Eid AH, El-Yazbi AF. Perirenal adipose tissue inflammation: novel insights linking metabolic dysfunction to renal diseases. Front Endocrinol. 2021;12:707126.
36. Wu C, Zhang H, Zhang J, Xie C, Fan C, Zhang H, et al. Inflammation and fibrosis in perirenal adipose tissue of patients with aldosterone-producing adenoma. Endocrinology. 2018;159:227–37.
37. Zhou G, Johansson U, Peng XR, Bamberg K, Huang Y. An additive effect of eplerenone to ACE inhibitor on slowing the progression of diabetic nephropathy in the db/db mice. Am J Transl Res. 2016;8:1339–54.
38. Rickard AJ, Morgan J, Bienvenu LA, Fletcher EK, Cranston GA, Shen JZ, et al. Cardiomyocyte mineralocorticoid receptors are essential for deoxycorticosterone/salt-mediated inflammation and cardiac fibrosis. Hypertension. 2012;60:1443–50.
39. Manno C, Campobasso N, Nardecchia A, Triggiani V, Zupo R, Gesualdo L, et al. Relationship of para- and perirenal fat and epicardial fat with metabolic parameters in overweight and obese subjects. Eat Weight Disord. 2019;24:67–72.
40. Lamacchia O, Nicastro V, Camarchio D, Valente U, Grisorio R, Gesualdo L, et al. Para- and perirenal fat thickness is an independent predictor of chronic kidney disease, increased renal resistance index and hyperuricaemia in type-2 diabetic patients. Nephrol Dial Transpl. 2011;26:892–8.
41. D'Marco L, Salazar J, Cortez M, Salazar M, Wettel M, Lima-Martinez M, et al. Perirenal fat thickness is associated with metabolic risk factors in patients with chronic kidney disease. Kidney Res Clin Pract. 2019;38:365–72.
42. Hung CS, Ho YL, Chang YY, Wu VC, Wu XM, Lee JK, et al. Twenty-four-hour urinary aldosterone predicts inappropriate left ventricular mass index in patients with primary aldosteronism. Sci World J. 2013;2013:294594.
43. Chang YY, Lee HH, Hung CS, Wu XM, Lee JK, Wang SM, et al. Association between urine aldosterone and diastolic function in patients with primary aldosteronism and essential hypertension. Clin Biochem. 2014;47:1329–32.
44. Hoppmann J, Perwitz N, Meier B, Fasshauer M, Hadaschik D, Lehnert H, et al. The balance between gluco- and mineralocorticoid action critically determines inflammatory adipocyte responses. J Endocrinol. 2010;204:153–64.
45. Guo C, Ricchiuti V, Lian BQ, Yao TM, Coutinho P, Romero JR, et al. Mineralocorticoid receptor blockade reverses obesity-related changes in expression of adiponectin, peroxisome proliferator-activated receptor-gamma, and proinflammatory adipokines. Circulation. 2008;117:2253–61.
46. Brown NJ. Contribution of aldosterone to cardiovascular and renal inflammation and fibrosis. Nat Rev Nephrol. 2013;9:459–69.
47. Shlomai G, Sella T, Sharabi Y, Leibowitz A, Grossman E. Serum potassium levels predict blood pressure response to aldosterone antagonists in resistant hypertension. Hypertens Res. 2014;37:1037–41.
48. Ghazi L, Dudenbostel T, Lin CP, Oparil S, Calhoun DA. Urinary sodium excretion predicts blood pressure response to spironolactone in patients with resistant hypertension independent of aldosterone status. J Hypertens. 2016;34:1005–10.
49. Siddiqui M, Judd EK, Jaeger BC, Bhatt H, Dudenbostel T, Zhang B, et al. Out-of-clinic sympathetic activity is increased in patients with masked uncontrolled hypertension. Hypertension. 2019;73:132–41.
50. Murabayashi M, Daimon M, Murakami H, Fujita T, Sato E, Tanabe J, et al. Association between higher urinary normetanephrine and insulin resistance in a Japanese population. PLoS ONE. 2020;15:e0228787.
51. Parasiliti-Caprino M, Obert C, Lopez C, Bollati M, Bioletto F, Bima C, et al. Association of urine metanephrine levels with cardiometabolic risk: an observational retrospective study. J Clin Med. 2021;10:1967.
52. Eisenhofer G, Peitzsch M. Laboratory evaluation of pheochromocytoma and paraganglioma. Clin Chem. 2014;60:1486–99.
53. Li P, Liu B, Wu X, Lu Y, Qiu M, Shen Y, et al. Perirenal adipose afferent nerves sustain pathological high blood pressure in rats. Nat Commun. 2022;13:3130.
54. Li M, Shi J, Sheng Y, Zhang Y, Wu T, Yang J, et al. Effect of focused power ultrasound-mediated perirenal fat modification on primary hypertension: protocol of a multicenter, randomized, double-blinded, sham-controlled study. Trials. 2023;24:221.
55. Sheu JY, Wang SM, Wu VC, Huang KH, Tseng CS, Lee YJ, et al. Estimated glomerular filtration rate-dip after medical target therapy associated with increased mortality and cardiovascular events in patients with primary aldosteronism. J Hypertens. 2023;41:1401–10.
56. Kobayashi H, Abe M, Nakamura Y, Takahashi K, Fujita M, Takeda Y, et al. Association between acute fall in estimated glomerular filtration rate after treatment for primary aldosteronism and long-term decline in renal function. Hypertension. 2019;74:630–8.

57. Chen JY, Huang KH, Lin YH, Chueh JS, Wang HY, Wu VC. Association of Dip in eGFR with clinical outcomes in unilateral primary aldosteronism patients after adrenalectomy. J Clin Endocrinol Metab. 2024;109:e965–e74.
58. Helal I, Fick-Brosnahan GM, Reed-Gitomer B, Schrier RW. Glomerular hyperfiltration: definitions, mechanisms and clinical implications. Nat Rev Nephrol. 2012;8:293–300.
59. Sanz-Gomez M, Manzano-Lista FJ, Vega-Martin E, Gonzalez-Moreno D, Alcala M, Gil-Ortega M, et al. Finerenone protects against progression of kidney and cardiovascular damage in a model of type 1 diabetes through modulation of proinflammatory and osteogenic factors. Biomed Pharmacother. 2023;168:115661.
60. Sun JY, Li C, Shen ZX, Zhang WC, Ai TJ, Du LJ, et al. Mineralocorticoid receptor deficiency in macrophages inhibits neointimal hyperplasia and suppresses macrophage inflammation through SGK1-AP1/NF-kappaB pathways. Arterioscler Thromb Vasc Biol. 2016;36:874–85.
61. Belden Z, Deiuliis JA, Dobre M, Rajagopalan S. The role of the mineralocorticoid receptor in inflammation: focus on kidney and vasculature. Am J Nephrol. 2017;46:298–314.
62. Zelicha H, Schwarzfuchs D, Shelef I, Gepner Y, Tsaban G, Tene L, et al. Changes of renal sinus fat and renal parenchymal fat during an 18-month randomized weight loss trial. Clin Nutr. 2018;37:1145–53.
63. Cuatrecasas G, Calbo M, Rossell O, Dachs L, Aguilar-Soler G, Coves MJ, et al. Effect of Liraglutide in different abdominal fat layers measured by ultrasound: the importance of perirenal fat reduction. Obes Facts. 2024;17:347–54.
64. Cuatrecasas G, De Cabo F, Coves MJ, Patrascioiu I, Aguilar G, Cuatrecasas G, et al. Dapagliflozin added to metformin reduces perirenal fat layer in type 2 diabetic patients with obesity. Sci Rep. 2024;14:10832.